Distance Measurements Near the Myosin Head-Rod Junction Using Fluorescence Spectroscopy

Murat Kekic,* William Huang,# Pierre D. J. Moens,* Brett D. Hambly,# and Cristobal G. dos Remedios*§
*Muscle Research Unit, Department of Anatomy and Histology, #Department of Pathology, and §Sydney Institute for Biomedical Research, The University of Sydney, Sydney 2006, Australia

ABSTRACT We reacted a fluorescent probe, *N*-methyl-2-anilino-6-naphthalenesulfonyl chloride (MNS-Cl), with a specific lysine residue of porcine cardiac myosin located in the S-2 region of myosin. We performed fluorescence resonance energy transfer (FRET) spectroscopy measurements between this site and three loci (Cys109, Cys125, and Cys154) located within different myosin light-chain 2s (LC2) bound to the myosin "head." We used LC2s from rabbit skeletal muscle myosin (Cys125), chicken gizzard smooth muscle myosin (Cys109), or a genetically engineered mutant of chicken skeletal muscle myosin (Cys154). The atomic coordinates of these LC2 loci can be closely approximated, and the FRET measurements were used to determine the position of the MNS-labeled lysine with respect to the myosin head. The C-terminus of myosin subfragment-1 determined by Rayment et al. ends abruptly after a sharp turn of its predominantly α-helical structure. We have constructed a model based on our FRET distance data combined with the known structure of chicken skeletal muscle myosin subfragment-1. This model suggests that the loci that bracket the head-rod junction will be useful for evaluating dynamic changes in this region.

INTRODUCTION

The myosin head has two distinct domains, a globular, active motor domain and a narrower neck region called the light-chain domain. A model of force generation (Rayment et al., 1993a; Spudich, 1994) proposes that the binding and hydrolysis of ATP results in the head being activated in a "pre-powerstroke" conformation. The motor domain then undergoes a conformational change when it binds strongly to actin. The light-chain domain then swings through an angle of approximately 45°, corresponding to a movement of 5–10 μm at the head-rod junction. Thus, this model proposes that the light-chain domain acts as a lever for the motor domain, amplifying the force-generating conformational change that occurs in the motor domain. Recent spin resonance spectroscopic data, from a probe bound to LC2, support the hypothesis that the light-chain domain is disordered during the entire contractile cycle, consistent with its swinging through large angles during contraction (Hambly et al., 1992).

Striated muscle is regulated by the thin filament-based troponin-tropomyosin system, whereas in smooth and nonmuscle tissue, force generation is regulated via phosphorylation of the myosin regulatory light chain (LC2) (Kendrick-Jones and Scholey, 1981). In cardiac (Malhotra et al., 1979) and skeletal muscle (Metzger and Moss, 1992; Sweeney et al., 1993), additional modulatory mechanisms may exist, for example, modulation by LC2. The mechanism by which LC2 regulates or modulates the myosin ATPase activity is not well understood.

LC2 has a M_r of ~20 kDa and is a member of the Ca^{2+}-binding regulatory protein superfamily. These proteins have a dumbbell-like shape and are characterized by strong structural homology to calmodulin (Meador et al., 1992) and troponin-C (Collins, 1991). In the crystal structure of S-1, the LC2 (Rayment et al., 1993b; Xie et al., 1994) wraps around and stabilizes the single α-helix of the MHC. The α-helix of the myosin heavy chain (MHC) in the light-chain binding domain undergoes a sharp bend of 40–90° at the center of the LC2-binding site. A highly conserved (invariant) proline (Pro840) is thought to demarcate the head-rod junction (Rimm et al., 1989). The proximity between LC2 and the putative head-rod junction suggests that these two structures may interact during force production (Miller and Reisler, 1985).

An experimental means of measuring movements between the LC domain (e.g., LC2) and the S-2 moiety would be valuable for testing molecular models. Fluorescence spectroscopy has a proven record for measuring distances in contractile proteins and would be appropriate in this context, provided that loci are available that can be specifically labeled. Hiratsuka and Uchida (1977) found that the fluorescent probe *N*-methyl-2-anilino-6-naphthalenesulfonyl chloride (MNS-Cl) selectively reacts with lysyl residues located close to the head-rod junction of porcine cardiac myosin. In the absence of divalent metal ions, porcine cardiac myosin contains two distinct Lys residues that react with MNS-Cl. However, in the presence of Ca^{2+}, a single different Lys residue reacts with the MNS-Cl probe (Hiratsuka and Uchida, 1980). The fluorophore is believed to be close to the head-rod junction, for which there is no known sequence. Its position has not been identified more specifically than within a 6600-Da chymotryptic S1-S2 linker

Received for publication 16 January 1996 and in final form 27 March 1996.

Address reprint requests to Dr. Murat Kekic, Muscle Research Unit, Department of Anatomy and Histology, The University of Sydney, Sydney 2006, Australia. Tel.: 61-2-3513209; Fax: 61-2-3512813; E-mail: rat@anatomy.su.oz.au.

0006-3495/96/07/40/08 $2.00

peptide of porcine cardiac myosin (Hiratsuka and Uchida, 1981). Hiratsuka (1981) found that the MNS probe was sensitive to actin binding.

In this study we have exchanged LC2, labeled with the fluorescent probe 5-iodoacetamidofluorescein (5-IAF), onto MNS-labeled porcine cardiac myosin. Fluorescence resonance energy transfer (FRET) was then performed between the donor-labeled site on the S-2 region of the MHC and the acceptor-labeled site on LC2. Thus, using the Förster theory of FRET, it is possible to establish the proximity of LC2 to the MNS site on S-2, thus bracketing the head-rod junction.

MATERIALS AND METHODS

Proteins and chemical reagents

ATP, papain, α-chymotrypsin, bovine thrombin, and proteinase-K were purchased from the Sigma Chemical Co. Cardiac myosin was prepared from the left ventricles of freshly slaughtered pig as described by Murakami et al. (1976), except for the addition of further protease inhibitors leupeptin, chymostatin, phenylmethylsulfonyl fluoride, and TLCK (10 mg/liter) to the washing and extraction buffers. Smooth muscle LC2 was prepared from the gizzards of freshly slaughtered chickens by the method of Grand and Perry (1983). Rabbit skeletal muscle LC2 was prepared using the method of Holt and Lowey (1975). Rabbit skeletal muscle actin was prepared from acetone powder by the method of Spudich and Watt (1971).

A mutant LC2 containing one Cys residue at position 154 (C125R) was also used. A chicken fast skeletal LC2 cDNA clone (expression vector: pLcIIFXMLC) (Reinach et al., 1986) was mutated by using oligonucleotide-primed site-directed mutagenesis as described previously (Boey et al., 1994). The endogenous Cys125 was substituted with an Arg (a conservative substitution found in chicken gizzard LC2 and chosen because it is likely to produce a functional LC2). The base change in the LC2 gene was confirmed by sequencing. The plasmid expressed a fusion protein consisting of a 31-residue peptide linked to the N-terminus of LC2 by a thrombin cleavage site. Removal of this fusion peptide was performed as described by Reinach et al. (1986) with modifications. C125R fusion peptide protein was dialyzed into thrombin digestion buffer (100 mM NaCl, 0.5 mM dithiothreitol (DTT), 40 mM Tris, pH 8.0). Bovine thrombin was suspended at 100 National Institutes of Health Units/ml, and digestion was carried out at 2 mg/ml protein, at 23°C in the presence of 1:40 v/v thrombin for 3 h. After cleavage, C125R was purified by Q-Sepharose (Pharmacia) anion exchange chromatography in 2 M urea, 50 mM Tris (pH 8.0), 0.5 mM DTT.

Labeling of MHC

All of the labeling steps were performed at 4°C unless otherwise specified. MNS-Cl and 5-IAF were purchased from Molecular Probes. A 12-fold molar excess of MNS-Cl was added to myosin (5 mg/ml), as described by Hiratsuka and Uchida (1977), in the presence of 2 mM Ca^{2+}. The reaction was terminated by the addition of 10 volumes of cold water and centrifuged at 6500 × *g* for 10 min. Myosin was redissolved in 0.5 M KCl, 2 mM $CaCl_2$, 40 mM Na-borate (pH 8.0) and dialyzed exhaustively. The extent of labeling was determined by the absorption difference between labeled and unlabeled myosin at 327 nm, using an extinction coefficient of 2.0×10^4 M^{-1} cm^{-1} (Hiratsuka and Uchida, 1977). The myosin concentration was established from its absorbance at 280 nm by using an extinction coefficient of 0.56 (Chock and Eisenberg, 1979). Labeling ratios were in the range of 0.59–1.0. The labeled myosin was designated as MNS-myosin.

Labeling of gizzard LC2 at Cys109

Lyophilized chicken gizzard LC2 was incubated in 6 M guanidine hydrochloride (GuHCl), 10 mM DTT, and 100 mM Tris (pH 8.0) for 2 h at 22°C. This was then dialyzed for 24 h at 4°C in 100 mM NaCl, 2 mM EDTA, and 20 mM imidazole and centrifuged at 130,000 × *g* for 30 min to remove denatured protein. Protein concentration was estimated by measuring the UV absorbance at 280 nm, using an extinction coefficient of 0.60 (Holt and Lowey, 1975). A 5 M excess of 5-IAF was added over the LC2 concentration and incubated for 40 min. The reaction was terminated by the addition of 100-fold excess of DTT over 5-IAF. Excess probe was removed by chromatography on Sephadex G-25 (Pharmacia) equilibrated with 0.2 mM DTT, 0.2 mM EDTA, and 0.15 M Na-phosphate (pH 7.0). The extent of labeling at Cys109 was determined at 495 nm, using an extinction coefficient of 5.47×10^4 M^{-1} cm^{-1} (Marsh and Lowey, 1980). As 5-IAF has a significant absorption at 280 nm, the concentration of LC2 was determined by using a standard Coomassie assay, (Bradford, 1976). We obtained labeling ratios between 0.79 and 1.08.

Labeling of Cys125

Cys125 of rabbit skeletal muscle LC2 was modified specifically with 5-IAF, using the method described by Katoh and Lowey (1989). LC2 (1–2 mg/ml) was reduced for 2 h at 22°C in 6 M GuHCl, 10 mM DTT, and 0.1 M Tris (pH 8.0) and dialyzed exhaustively against 0.1 M NaCl, 2 mM EDTA, 20 mM imidazole (pH 7.0) before labeling with 5 M excess fluorophore for 45 min at 4°C. The sample was then immediately passed through a Sephadex G-25 column (equilibrated in 0.2 mM DTT, 0.2 mM EDTA, 0.15 M Na-PO_4, pH 7.0) to remove the excess probe. To remove unlabeled and double-labeled LC2, it was further purified by passage through a Q-Sepharose column equilibrated in the same buffer. Unlabeled LC2 eluted with the void volume, and labeled LC2 eluted with a linear gradient to 0.4 M Na-PO_4. The first eluted peak contained single-labeled LC2 and the second double-labeled LC2. Fractions containing single-labeled LC2 were pooled for exchange onto myosin.

Labeling of Cys154

Mutant chicken fast skeletal myosin LC2 (C125R) containing one Cys at position 154 was reduced and labeled, using the same conditions and procedures described for rabbit skeletal myosin LC2, except that 2 M urea was included in the labeling buffer.

Exchange of labeled LC2 onto MNS-labeled myosin

MNS-myosin (2 mg/ml) was incubated for 15 min at 37°C in buffer free of Ca^{2+} or Mg^{2+} (0.5 M NaCl, 2 mM EDTA, 5 mM ATP, and 40 mM Tris, pH 8.0) to remove native LC2 (Wikman-Coffelt et al., 1979). The reaction was terminated by precipitating myosin in 10 volumes of ice cold water and centrifuged at 40,000 × *g* for 15 min at 4°C. Myosin was redissolved in 0.5 M NaCl, 5 mM $MgCl_2$, and 50 mM Tris (pH 8.0). A 3 M excess of labeled LC2 was added to MNS-myosin, and the mixture was incubated for 12 h at 4°C. Unexchanged LC2 was removed by the addition of 10 volumes of ice-cold water; centrifuged at 40,000 × *g* for 15 min; dissolved in 0.5 M KCl, 2 mM $MgCl_2$, 40 mM Na-borate (pH 8.0); and repeated. Denatured proteins were removed by centrifugation at 130,000 × *g* for 60 min. The amount of LC2 exchanged onto myosin was quantified by UV/Vis spectroscopy and Coomassie protein assays, assuming that the concentration of 5-IAF (determined from its absorbance peak at 495) was equivalent to the amount of acceptor-labeled LC2 exchanged onto the MHC. MHC:LC2 ratios of 0.72–1.0 were achieved. The hybrid myosins are referred to as MNS-109, MNS-125, and MNS-154.

Myosin ATPase activities at low ionic strength (33 mM KCl) in the presence and absence of a 2 M excess of F-actin were measured by using a pH stat as described elsewhere (dos Remedios and Barden, 1977). All

myosin ATPase rates were within ±10% of the control (unlabeled myosin with native LC2s) activities (data not shown).

Fluorescence measurements

The fluorescence spectra were recorded with an SLM 8000 photon-counting spectrofluorimeter operated in ratio mode with a rhodamine standard as described previously (Barden and dos Remedios, 1984). Samples were placed in cuvettes, and the temperature was regulated at 20°C and constantly stirred. The protein concentration in all samples was adjusted to approximately 1 mg/ml in 0.5 M KCl, 2 mM $MgCl_2$, and 40 mM Na-borate (pH 8.0). Excitation wavelength for all samples was at 330 nm, and the emission spectra were recorded in the range of 380–480 nm.

FRET analysis

The efficiency of FRET between a donor and an acceptor probe was calculated according to the Förster (1965) equation:

$$E = R_0^6/(R_0^6 + R^6) \quad (1)$$

where

$$R = 9.78 \times 10^3 (Jn^{-4}k^2Q_D)^{1/6}, \quad (2)$$

where E is the efficiency of resonance energy transfer; R_0 is the Förster distance between donor and acceptor probe at which the efficiency is 50%; R is the distance separating the donor and acceptor probes; k^2 is the dipolar orientation factor and is assumed to be equal to 2/3 (see dos Remedios, 1977; dos Remedios and Moens, 1995, for a detailed discussion of this assumption); n is the refractive index of the medium; Q_D is the quantum yield of the donor; and J is the overlap integral between the emission spectrum of the donor $[F_D(l)]$ and the absorption spectrum of the acceptor $[eA(l)]$ in M^{-1} cm^{-1}. J is defined as

$$J = \int F_D(l) eA(l) l^4 dl^4 \Big/ \int F_D(l) dl. \quad (3)$$

E is calculated from the equation

$$E = 1 - (F_{da}/F_d), \quad (4)$$

where F_{da} and F_d are the fluorescence intensities of the donor in the presence and absence of acceptor, respectively.

RESULTS

Labeling a specific lysine in S-2

In the absence of free Ca^{2+} we confirmed the observations of Hiratsuka and Uchida (1977), who reported a 2:1 labeling stoichiometry of MNS:myosin, i.e., one label for each of the two strands of the porcine cardiac MHC. However, when this myosin was labeled in the presence of free Ca^{2+}, the MNS:myosin ratio was ~1.0. We confirmed the requirement for Ca^{2+} to achieve a stoichiometry of one MNS label per myosin molecule. In a series of six separate experiments, the labeling ratios varied in the range 0.59–1.0 moles of MNS per MHC. Thus, Hiratsuka's procedure achieves one mole of label per myosin, i.e., only one label for every two MHCs in the presence of Ca^{2+}.

Comparison of the near-UV spectra for single (*curve b* in Fig. 1) and double (*curve a* in Fig. 1) MNS-labeled myosins

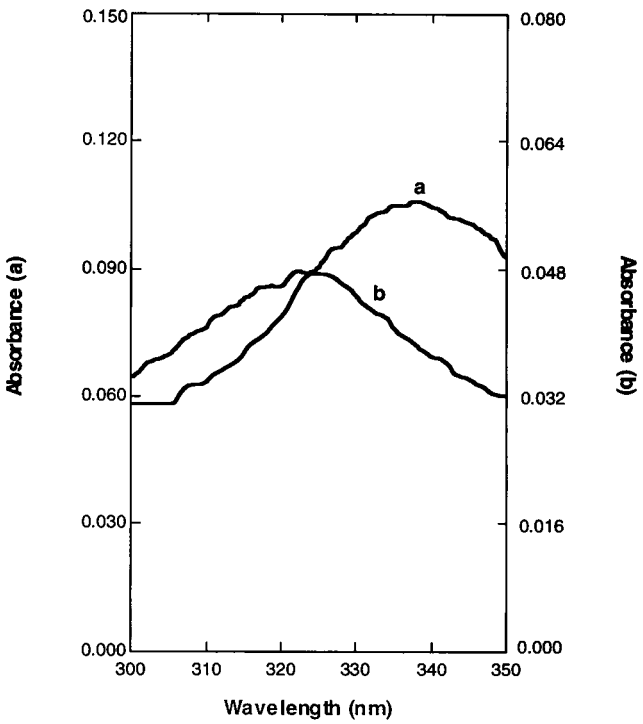

FIGURE 1 Near-UV absorption spectra of porcine cardiac myosin labeled with a 12-molar excess of MNS-Cl in the absence (*curve a*) and presence (*curve b*) of 2 mM Ca^{2+}. Note the blue shift of the spectrum obtained when myosin is labeled in the presence of Ca^{2+}.

reveals a blue shift of the absorbance of the single-labeled preparations (peak occurs at 327 nm). This suggests that the solvent environment of this label is more hydrophobic than for the double-labeled myosin, where the peak occurs at 335–340 nm.

In the presence of Ca^{2+} the MNS probe reported by Hiratsuka was located in the S-2 region of myosin (Hiratsuka and Uchida, 1981). We confirmed this by producing standard HMM and S-1 fragments of myosin by using chymotrypsin and papain, respectively. The fluorescence emission spectra of MNS-labeled HMM and S-1 are illustrated in Fig. 2. This comparison suggests that essentially all of the fluorescence resides in HMM.

Preliminary experiments with myosins from other species produced different results. When we labeled bovine cardiac myosin with a 12-fold excess of MNS-Cl, the myosin:label stoichiometry was in excess of 2:1. A similar result was obtained by using myosin isolated from rabbit skeletal muscle. These observations suggests that pig heart myosin may have either a unique primary structure or a unique conformation due to its interaction with other ligands (Hiratsuka, personal communication).

Energy transfer between MNS-myosin and LC2 5-IAF-labeled at Cys109, Cys125, or Cys154

Fig. 3 illustrates the corrected fluorescence spectra of myosin labeled with a single MNS probe (MNS-myosin) in the

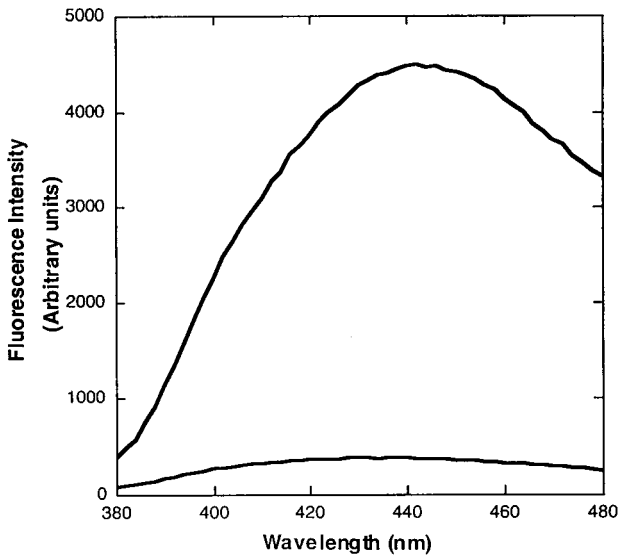

FIGURE 2 Fluorescence emission spectra of MNS-myosin digested to HMM (*top curve*) and S-1 (*bottom curve*). Buffer conditions were 0.5 mM KCl and 10 mM Tris (pH 7.0). The instrument was operated in multiscan mode, acquisition time was 1 s, excitation and emission monochromator slits were set at 4 nm, and excitation wavelength was 330 nm. The concentrations of both HMM and S-1 were 0.73 μM.

absence (*solid curve*) and presence (*dashed curve*) of 5-IAF acceptor located at Cys109 of gizzard LC2. The curves have been normalized for protein concentration and for the ratio of labeling of the acceptor. The MNS-myosin has a peak fluorescence intensity at 438 nm. In this sample, the FRET efficiency was 0.58. Transfer efficiencies between the donor and acceptor probes were determined by using three separately prepared samples of MNS-myosin exchanged with 5-IAF-labeled LC2 (Table 1). The measurements yielded an average transfer efficiency of 0.62.

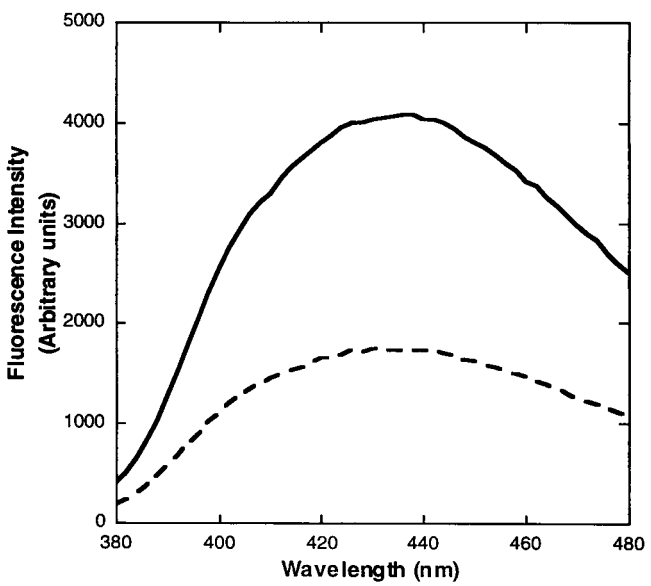

FIGURE 3 Corrected fluorescence emission spectra of MNS-myosin (*solid line*) and MNS-5-IAF-Cys109 (*broken line*). The acquisition time was 1 s, and excitation and emission monochromator slits were both set at 4 nm. The excitation wavelength was 330 nm, and fluorescence quench was monitored at 438 nm. The FRET efficiency of this sample was 0.58.

Precisely equivalent experiments were performed by using the 5-IAF acceptor bound to rabbit skeletal myosin LC2 (Cys125) and to a chicken skeletal muscle myosin mutant LC2 (Cys154). The corresponding FRET efficiencies are summarized in Table 1.

The distances between the donor and acceptor probes were calculated with Eq. 1. The parameters used in calculating the R_0 are summarized in Table 2, where J was calculated from the absorption-emission spectra of the MNS-labeled myosin. R_0 for the probe pair MNS-Cl (donor)/5-IAF (acceptor) was calculated to be 2.68 nm. The distance values (R) were then calculated from the observed FRET efficiencies and are summarized in Table 1. The mean distances between the MNS donor and 5-IAF acceptors were 2.48 nm (Cys109), 2.31 nm (Cys125), and 2.56 nm (Cys154).

DISCUSSION

Structure of the S-1-S-2 portion of myosin

The structure of the α-carbon backbone of S-1 and its associated myosin light chains is now well defined; this is shown in Fig. 4 *a*. The truncated myosin heavy chain illustrated in Fig. 4 *b* has approximately the same orientation as the S-1 shown in Fig. 4 *a*. It commences at Val700 and is traced to its termination at Lys843. Thus, residues 1 to 700 are not visualized in this figure, some of which overlaps this region. The important features of the heavy-chain structure are the extended α-helix (green), which begins in the so-called motor domain and extends into the "light-chain" domain as a nearly linear structure.

First LC1 and then LC2 are "wrapped" around this helix. The sequence of the cognate peptide that binds to Ca^{2+}-binding regulatory proteins exhibits a characteristic motif: the IQ motif (Xie et al., 1994). Such motifs occur within the MHC sequences that bind both LCs, although the motif for LC2 is significantly altered. The target sequences of calm-

TABLE 1 Summary of the FRET data

Location of acceptor probe on LC2	A/D	Corrected E	R 2/3 (nm)	Mean R (nm)
Cys109	0.94	0.58	2.54	2.48
	0.81	0.61	2.49	
	1.05	0.66	2.40	
Cys125	0.72	0.71	2.31	2.31
Cys154	1.00	0.50	2.68	2.56
	1.06	0.63	2.45	

In all experiments the donor (D) was located on a Lys of myosin S-2. E is the efficiency of energy transfer calculated from Eq. 4; R is the distance between the donor and acceptor (A) probes calculated using Eq. 1; R_0 = 2.68 nm. We have assumed that the probes were able to freely precess and therefore have an orientation factor (κ^2) value of 2/3.

TABLE 2 A summary of the parameters used in calculating the Förster distance (R_0)

Donor	Acceptor	J	n	κ^2	Q_D	R_0 (nm)
MNS-Cl	5-IAF	1.97×10^{-14}	1.33	0.67	0.10	2.68

Q_D was obtained from Hiratsuka and Uchida (1980).

odulin-binding peptides and the binding site for the alkali light chains of myosin all form single straight α-helices. However, the binding of LC2 to the MHC differs from this in that there has been an "insertion" of the central three residues into the IQ motif (829–831). This insertion causes it to undergo a 40–90° bend, depending on the myosin isotype (Rayment et al., 1993b; Xie et al., 1994).

The heavy chain continues for 12 more residues beyond the bend within LC2. These form three turns of an α-helix before terminating at Lys843. This C-terminal α-helix now points in a direction nearly at right angles to the axis of the head. When Rayment et al. (1993a) fitted the F-actin–S-1 model into the context of the myofibril, this C-terminal helix pointed toward the M-line and represented an appropriate mechanical arrangement for S-1 to apply tension to the rod portion of the myosin. Thus, the model of Rayment et al. predicts that the S-2 segment continues in the direction indicated in Fig. 4. The flexible hinge of the MHC at Pro840, believed to constitute the head-rod junction (Rimm et al., 1989), is four residues beyond the C-terminus of the S-1 crystal structure.

A specific labeling site on myosin

The generation of S-1 by proteolytic digestion produces several peptides that lie between S-1 and S-2. One of these is a 6.6-kDa "linker" peptide that Hiratsuka identified as containing the MNS-sensitive lysine. Our experiments confirmed observations by Hiratsuka and his colleagues (Hiratsuka, 1981; Hiratsuka and Uchida, 1977, 1980), namely that 1 mole of the MNS label is incorporated into each mole of porcine cardiac myosin when the reaction is carried out in the presence of excess Ca^{2+}. In the absence of added Ca^{2+}, two moles of MNS are incorporated per myosin, resulting in characteristically different UV absorbance and fluorescence emission spectra. Hiratsuka concluded that different loci are labeled in the presence and absence of Ca^{2+}. Our results demonstrate that the 1:1 labeling in the presence of Ca^{2+} is not a general property of striated myosins because a $\gg$1:1 ratio was achieved by using bovine cardiac or rabbit skeletal muscle myosins.

The MNS label was localized to the S-2 region of the MHC, and our data show that essentially all of the fluorescence intensity is associated with HMM rather than S-1. This is consistent with Hiratsuka's observation (Hiratsuka, 1981) that the MNS-labeled lysine is located in the 6.6-kDa S-2 fragment.

The problem of one donor and two acceptors

Each mole of LC2 may exchange at two possible sites on myosin. This exchange may be random or may involve positive or negative cooperativity. Wagner and Weeds (1977) reported that LC2 does not exchange equally onto both heads and concluded that the exchange exhibited negative cooperativity. The maximum level of exchange in our experiments was about 1 mole of label per mole of myosin, which is consistent with the conclusion of these authors. Thus it is likely that only a very small proportion of myosin molecules will contain two acceptors.

In the event that myosin does contain two acceptors, the distance calculations can be modified to take this circumstance into account. The equation for calculating distances in multiacceptor systems is

$$\sum_n (R_0^6/R_n^6) = (E^{-1} - 1)^{-1}, \quad (5)$$

where n is the number of acceptors. For two equidistant acceptors the equation for the distance between the probes reduces to

$$R = R_0(2)^{1/6}(E^{-1} - 1)^{1/6}. \quad (6)$$

For one donor and one acceptor, the calculated distances (R) were 2.48, 2.31, and 2.56 nm for the Cys109, Cys125, and Cys154, respectively. If we assume that all of our donors are equidistant from two acceptors then, using Eq. 6, the distances increased to 2.78, 2.59, and 2.87 nm, respectively. The greatest margin of error in these experiments, assuming all myosin molecules contain two acceptors, would be an underestimation of the distances by 12%. Within the context of our experiments, this level of error would not alter our conclusions.

Modeling the FRET distances between the S-2 lysine and three LC2 cysteines

Having confirmed the label specificity reported by Hiratsuka and his colleagues, we located the MNS probe in space by reference to the known crystal structure of chicken skeletal myosin S-1. MNS-labeled lysine was used as a donor in three separate experiments where acceptor probes were placed on Cys109 (from chicken gizzard smooth muscle myosin), Cys125 (from rabbit skeletal fast muscle myosin), and Cys154 (a site-directed mutant of chicken skeletal fast muscle myosin). The distances were modeled by locating the probes on the α-carbon backbone of the structure of Rayment et al. (1993b). Residue 109 from gizzard LC2 corresponds to Val103 of the chicken skeletal sequence, based on the sequence alignment of Collins (1991). It would have been ideal to have known the coordinates of the amino acid side chains of our labeled residues. These coordinates for Cys125 and Cys154 were kindly provided by Ivan Rayment (personal communication), but because the crystal structure residue corresponding to Cys109 was a Val, this side-chain coordinate could not be used.

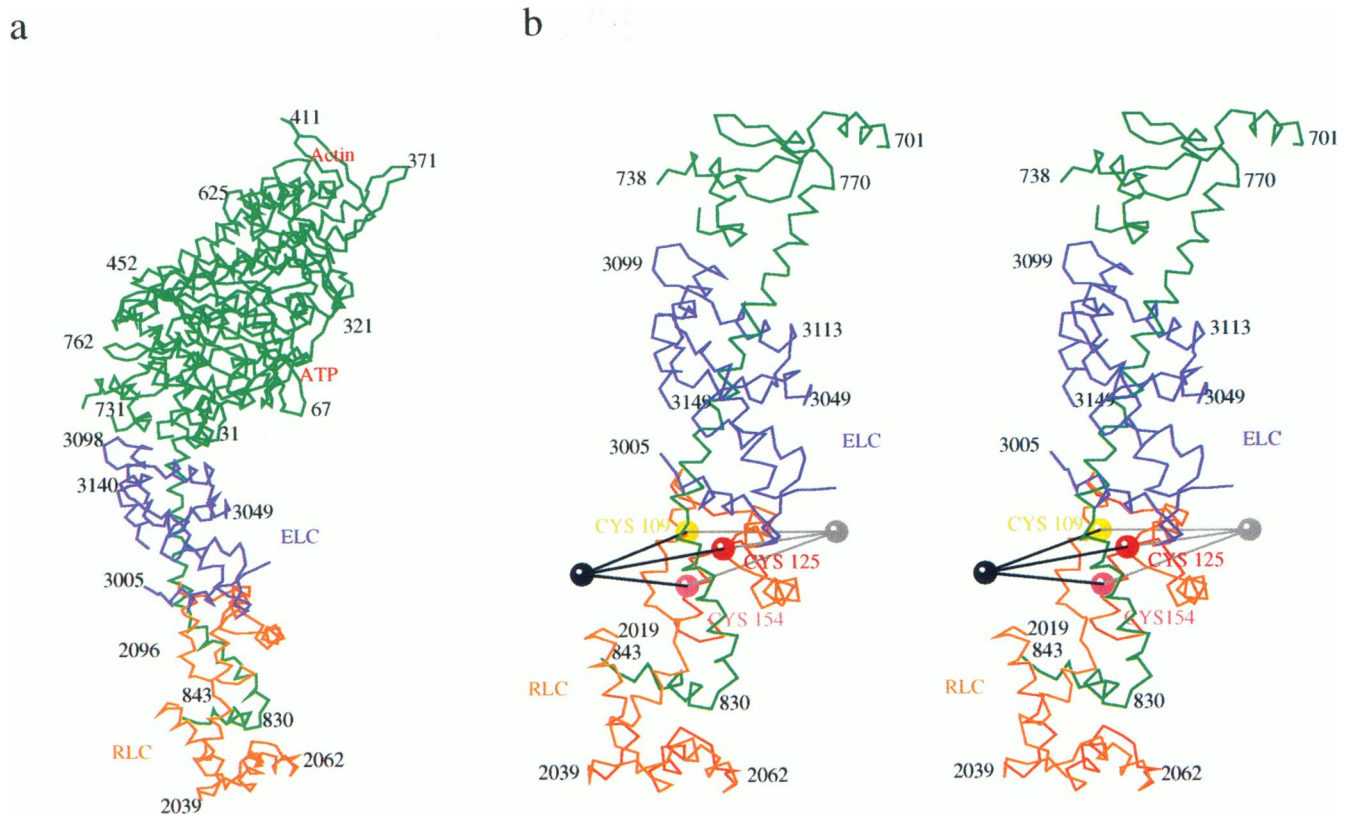

FIGURE 4 The left panel illustrates the complete crystal structure of chicken skeletal muscle myosin S-1 (*a*). The myosin heavy chain is shown in green, LC1 is shown in blue, and LC2 in orange. The panel on the right is a stereo pair view of the light-chain domain of S-1 (only residues 701–843 are illustrated). The three acceptor labels (at Cys109, Cys125, and Cys154) are superimposed on the LC2 α-carbon chain. The MNS donor probe is located at either of the mirror image positions illustrated by the black and grey spheres. The software used for this figure was RasMac version 2.5 ucb and Mage version 4.2.

Errors that occur because of the length of the amino acid side chains and the size of the probes themselves may not necessarily be significant. The distance between the α-carbons of Cys125 and Cys154 in the crystal structure is 1.98 nm, whereas the distance reported by us using FRET was 1.97 nm (Boey et al., 1994), i.e., in good agreement for such a short distance.

Several considerations must be taken into account when estimating the location of the α-carbon of the MNS-labeled lysine. The structures of the probes were obtained by energy minimization using Cerius^2 software. 5-IAF has a maximum cord of 0.95 nm. The maximum cord of the MNS probe was 1.15 nm. We can estimate the position of the MNS-labeled lysine by a sphere centered at the MNS locus with a diameter of 1.15 nm.

In Fig. 4 *b* the three α-carbons are colored yellow (Cys109), red (Cys125), and pink (Cys154), and we assumed that the probes can freely precess around these loci. The model of the FRET distances shows there are two possible solutions for the position of the MNS label, the one indicated by the black sphere and its mirror image (*grey sphere*). We calculated the distance from the last residue identified in the Rayment structure (Lys843) to the black and grey spheres to be 3.0 and 4.5 nm, respectively. This result favors the position of the MNS label represented by the black sphere, because it is closer to the C-terminus of the MHC.

Allosteric effects of LC2

Miller and Reisler (1985) found that the binding of F-actin inhibited both the papain and chymotryptic digestion of HMM at the S1-S2 junction, yielding "long" and "short" S-1 fragments, respectively. No inhibition occurred when the HMM contained a degraded (17 or 14 kDa) LC2. However, when the LC2 was degraded to 18 kDa, digestion was similar to that obtained in HMM using an intact LC2. Thus, removal of the first seven N-terminal residues of LC2 has little impact on the chymotryptic susceptibility of the S1-S2 junction, whereas the removal of a further 11 (or more) residues renders LC2 incapable of interacting with this region. The first 18 residues of LC2 are not shown in the Rayment S-1 structure, because these residues are believed to be flexible. The data of Miller and Reisler suggest that the first 18 residues of LC2 "protect" the head-rod junction cleavage sites in the presence of actin. These data may be consistent with those of Hiratsuka, who showed that

the S-2-bound MNS probe becomes "buried" in the presence of actin. The conformational changes induced by actin binding that are associated with proteolytic protection and burial of the MNS probe may be the same. Our FRET data support this hypothesis by placing the MNS probe close to the C-terminus of the MHC.

The structural implications of our findings can best be understood by reference to a stylized cartoon of myosin structure (Fig. 5). The model of S-1 proposed by Rayment et al. (1993a) clearly implicates two "hinges" (indicated by the "screw heads" in this figure). Clear details are provided for a putative movement of the so-called S-1 motor domain (indicated by the grey arc) relative to the light-chain domain to which LC1 and LC2 are bound. The three probe loci on LC2 are shown as black spheres, and the MNS label site is shown as a white sphere in Fig. 5. Implicit in the model of Rayment et al. is a second hinge, which enables the light-chain domain of S-1 to change its attitude (indicated by the black arc) relative to S-2. Now that we have established a framework for locating the MNS site, we intend to proceed to examine the effects of F-actin binding. It remains to be seen whether this movement can be detected in solution.

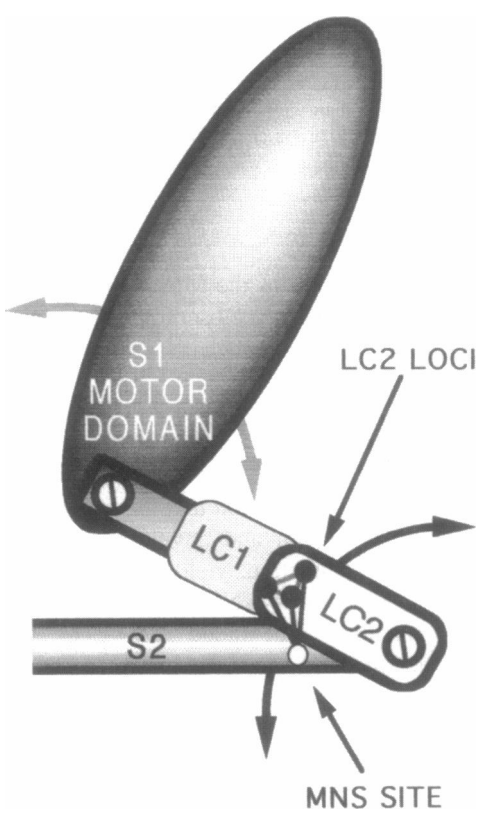

FIGURE 5 This cartoon depicts the globular motor domain "hinged" onto the light-chain domain of S-1. The light-chain domain binds both LC1 (*shaded*) and LC2 (*unshaded*), which extends to cover a second "hinge" (indicated by the screw head) at the junction of S-1 and S-2. The three LC2 label loci are shown as black spheres, and the MNS site is drawn as a white sphere. The black arc with arrowheads indicates possible movements that may be detected at this second "hinge" by using the LC2-MNS loci.

CONCLUSION

Based on the Rayment model of S-1, our FRET data are consistent with the C-terminus continuing in the direction indicated by these authors. Current theories on the mechanism whereby myosin develops force and is regulated rely on hinges such as the one adjacent to LC2. Therefore, the establishment of loci on S-2 and LC2 is an important first step in detecting movements at this hinge. Experiments are now in progress to determine whether our MNS-LC FRET distances are sensitive to the binding of ATP in both the presence and absence of F-actin.

We are grateful to Ivan Rayment for providing the atomic coordinates of the Cys residues of LC2. We thank Nicole Bordes (VisLab, University of Sydney) for her assistance with Cerius^2. We are grateful to Woy Woy Abattoirs for providing the pig hearts.

This research was supported by grants from the National Health and Medical Research Council of Australia and from the Ramaciotti Foundations.

REFERENCES

Barden, J. A., and C. G. dos Remedios. 1984. The environment of the high-affinity cation binding site on actin and the separation between cation and ATP sites as revealed by proton NMR and fluorescence spectroscopy. *J. Biochem.* 96:913–921.

Boey, W., W. Huang, B. Bennetts, J. Sparrow, C. G. dos Remedios, and B. D. Hambly. 1994. Fluorescence resonance energy transfer within the regulatory light chain of myosin. *Eur. J. Biochem.* 219:603–610.

Bradford, M. M. 1976. A rapid and sensitive method for the quantitation of microgram quantities of protein utilising the principle of protein-dye binding. *Anal. Biochem.* 72:248–254.

Chock, S. P., and E. Eisenberg. 1979. The mechanism of skeletal muscle myosin ATPase. I. Identity of the myosin active sites. *J. Biol. Chem.* 254:3229–3235.

Collins, J. H. 1991. Myosin light chains and troponin C: structural and evolutionary relationships revealed by amino acid sequence comparisons. *J. Muscle Res. Cell Motil.* 12:3–25.

dos Remedios, C. G., and J. A. Barden. 1977. Effects of Gd(III) on G-actin: Inhibition of polymerization of G-actin and activation of myosin ATPase activity by Gd-G-actin. *Biochem. Biophys. Res. Commun.* 77: 1339–1346.

dos Remedios, C. G., and P. D. J. Moens. 1995. Fluorescence resonance energy transfer spectroscopy is a reliable "ruler" for measuring structural changes in proteins—dispelling the problem of the unknown orientation factor. *J. Struct. Biol.* 115:175–185.

Förster, Th. 1965. Action of light and organic crystals. *In* Modern Quantum Chemistry. O. Sinanolglu, editor. Academic Press, New York. 93–137.

Grand, R. J. A., and S. V. Perry. 1983. Preparation of the alkali and P light chains of chicken gizzard myosin. *Biochem. J.* 211:267–272.

Hambly, B. D., K. Franks, and R. Cooke. 1992. Paramagnetic probes attached to a light chain on the myosin head are highly disordered in active muscle fibres. *Biophys. J.* 63:1306–1313.

Hiratsuka, T. 1981. Actin-induced conformational changes around the reactive fluorescence-labeled lysyl residues located in the subfragment-1/subfragment-2 link region of cardiac myosin. *J. Biol. Chem.* 256: 10645–10650.

Hiratsuka, T., and K. Uchida. 1977. Selective release of light chain-2 from pig cardiac myosin by chemical modification of specific lysyl residues with *N*-methyl-2-anilinonaphthalene-6-sulfonyl chloride. *J. Biochem.* 82:983–990.

Hiratsuka, T., and K. Uchida. 1980. Lysyl residues of cardiac myosin accessible to labeling with a fluorescent reagent, *N*-methyl-2-anilinonaphthalene-6-sulfonyl chloride. *J. Biochem.* 88:1437–1448.

Hiratsuka, T., and K. Uchida. 1981. Localisation and isolation of peptides in cardiac myosin that contain the lysyl residues accessible to labeling with a fluorescent reagent, *N*-methyl-2-anilinonaphthalene-6-sulfonyl chloride. *J. Biochem.* 89:111–123.

Holt, J. C., and S. Lowey. 1975. An immunological approach to the role of the low molecular mass subunits in myosin. II. Interaction of myosin and its subfragments with antibodies to the light chains. *Biochemistry.* 14: 4609–4620.

Kendrick-Jones, J., and J. M. Scholey. 1981. Myosin-linked regulatory systems. *J. Muscle Res. Cell Motil.* 2:347–372.

Lowey, S., G. S. Waller, and K. M. Trybus. 1993. Skeletal muscle myosin light chains are essential for physiological speeds of shortening. *Nature.* 365:454–456.

Malhotra, A., S. Huang, and A. Bhan. 1979. Subunit function in cardiac myosin: effect of removal of LC2 (18000 molecular weight) on enzymatic properties. *Biochemistry.* 18:461–467.

Marsh, D. J., and S. Lowey. 1980. Fluorescence energy transfer in myosin subfragment-1. *Biochemistry.* 19:774–784.

Meador, W. E., A. R. Means, and F. A. Quiocho. 1992. Target enzyme recognition by calmodulin: 2.4 Å structure of a calmodulin-peptide complex. *Science.* 257:1251–1255.

Metzger, J. M., and R. L. Moss. 1992. Myosin light chain 2 modulates calcium-sensitive cross-bridge transitions in vertebrate skeletal muscle. *Biophys. J.* 63:460–468.

Miller, L., and E. Reisler. 1985. Light chain dependant effects of actin binding on the S-1/S-2 swivel in myosin. *J. Mol. Biol.* 182:271–279.

Murakami, U., K. Uchida, and T. Hiratsuka. 1976. Cardiac myosin from pig heart ventricle. *J. Biochem.* 80:611–619.

Rayment, I., H. M. Holden, M. Whittaker, C. B. Yohn, M. Lorenz, K. C. Holmes, and R. A. Milligan. 1993a. Structure of the actin-myosin complex and its implications on muscle contraction. *Science.* 261: 58–65.

Rayment, I., W. R. Rypniewski, K. Schmidt-Base, R. Smith, D. R. Tomchick, M. M. Benning, D. A. Winklemann, G. Wesenberg, and H. M. Holden. 1993b. Three-dimensional structure of myosin subfragment-1: a molecular motor. *Science.* 261:50–58.

Reinach, F. C., K. Nagai, and J. Kendrick-Jones. 1986. Site directed mutagenesis of the regulatory light-chain Ca^{2+}/Mg^{2+} binding site and its role in hybrid myosins. *Nature.* 322:80–83.

Rimm, D. L., J. H. Sinnard, and T. D. Pollard. 1989. Location of the head-tail junction of myosin. *J. Cell Biol.* 108:1783–1789.

Spudich, J. A. 1994. How molecular motors work. *Nature.* 372:515–518.

Spudich, J. A., and S. Watt. 1971. The regulation of rabbit skeletal muscle contraction. I. Biochemical studies of the interaction of tropomyosin-troponin complex with actin and the proteolytic fragments of myosin. *J. Biol. Chem.* 246:4866–4871.

Sweeney, H. L., B. F. Bowman, and J. T. Stull. 1993. Myosin light chain phosphorylation in vertebrate striated muscle: regulation and function. *Am. J. Physiol.* C1085–C1095.

Uyeda, T. Q. P., and J. A. Spudich. 1993. A functional recombinant myosin II lacking a regulatory light chain-binding site. *Science.* 262:1867–1870.

Wagner, P. D., and A. G. Weeds. 1977. Studies on the role of the myosin alkali light chains. Recombination and hybridisation of light chains and heavy chains in subfragment-1 preparations. *J. Mol. Biol.* 109:455–470.

Wikman-Coffelt, J., S. Srivastava, and D. T. Mason. 1979. Dissociation and reassociation of rabbit skeletal muscle myosin. *Biochimie.* 61: 1309–1314.

Xie, X., D. H. Harrison, I. Schlichtling, R. M. Sweet, V. N. Kalabokis, A. G. Szent Gyorgyi, and C. Cohen. 1994. Structure of the regulatory domain of scallop myosin at 2.8 Å resolution. *Nature.* 368:306–312.